Studies on Geranylgeranylacetone Selectively Binds to the HSP70 of *Helicobacter Pylori* and Alters its Coccoid Morphology

by

Ewa Grave

Department of Life Science

Graduate School of Engineering Science

Akita University

March 2016

Contents

List of publications

Papers Relevant and Related to the Present Study

1. Haga A, Okamoto T, Yamada S, Kubota T, Sanpei A, Takahashi S, Nakayama M, Nagai M, Otaka M, Miyazaki T, Nunomura W, **Grave E**, Itoh H.: Zinc-L-Carnosine Binds to Molecular Chaperone HSP70 and Inhibits the Chaperone Activity of the Protein. *J Biochemistry*. **154**, 249-56. (2013)

2. Tsuji N, Fukuda K, Nagata Y, Okada H, Haga, Hatakeyama S, Yoshida S, Okamoto T, Hosaka M, Sekine K, Ohtaka K, Yamamoto S, Otaka M, **Grave E**, Itoh H.: AhR activation mechanisms by molecular chaperone HSP90. *FEBS Open Bio* **4**, 796-803 (2014)

3. **Grave E**, Yokota S, Yamamoto S, Tamura A, Ohtaki-Mizoguchi T, Yokota K, Oguma K, Fujiwara K, Ogawa N, Okamoto T, Otaka M, Itoh H.: Geranylgeranylacetone selectively binds to the HSP70 of *Helicobacter pylori* and alters its coccoid morphology. *Scientific Reports* **5**:13738. doi: 10.1038/srep13738. (2015)

4. Okamoto T, Ishida R, Yamamoto H, Tanabe-Ishida M, Haga A, Takahashi H, Takahashi K, Goto D, **Grave E**, Itoh H.: Functional structure and physiological functions of mammalian wild-type HSP60. *Archives Biochemistry and Biophysics*. **586**, 10-19 (2015)

5. Hatakeyama S, Kafuku M, Okamoto T, Kakizaki Y, Shimasaki N, Fujie N, Takahashi S, Nakayama M, Tagawa H, Komatsuda A, **Grave E**, Wakui H, Itoh H: Studies on the anticancer mechanisms of the Natto extract.
Journal of the Society Materials Engineering for Resources. in press (2016)

Chapter I

General Introduction

1.1 Molecular chaperone

Heat-shock proteins (HSPs) are present in all living organisms; their presence has been detected both in simple monocellular species and in highly developed vertebrates, including humans [1]. The presence of HSP-coding genes was described for the first time in 1962 [2], but the proteins themselves were discovered in 1974 in Drosophila melanogaster [3]. The name of heat-shock proteins originated from the observation that their concentration increases following exposure to thermal stress. However, it has been found that HSPs are produced in several other risky situations, such as oxidative stress, exposure to chemical agents, biological agents (viral infections) or physical agents (UV radiation), a disturbed blood supply or insufficient nutrition [4]. In such situations the proteins protect cells and promote reparative processes in the damaged proteins [5]. Therefore, HSPs are sometimes thought to be chaperone proteins, even though many of them also function as proteases, participating in eliminating the damaged proteins.

Most proteins must fold into defined three-dimensional structures to gain functional activity. But in the cellular environment, newly synthesized proteins are at great risk of aberrant folding and aggregation, potentially forming toxic species. To avoid these dangers, cells invest in a complex network of molecular chaperones, which use ingenious mechanisms to prevent aggregation and promote efficient folding. Because protein molecules are highly dynamic, constant chaperone surveillance is required to ensure protein homeostasis (proteostasis). Recent advances suggest that an age-related decline in proteostasis capacity allows the manifestation of various protein-aggregation diseases, including Alzheimer's disease and Parkinson's disease. Interventions in these and numerous other pathological states may spring from a detailed understanding of the pathways underlying proteome maintenance.

In the current model, polypeptide chains are thought to explore funnel-shaped potential energy surfaces as they progress, along several downhill routes, towards the native structure (Fig. 1) [6].

Mechanisms of proteostasis impairment. Observations in cellular and organismal models indicate that chronic production of misfolded and aggregated proteins compromises central functions of the proteostasis network (PN), including the capacity of cells to fold proteins, clear misfolded pro-teins (Fig. 2A, B) and respond to conformational stress by upregulating PN machinery (Fig. 2C). How exactly the aberrant proteins target the PN is not clear in most cases, but it is plausible that they unduly occupy, sequester, or otherwise functionally impair PN components, rendering them unavailable for use by other clients (chaperone titration). These clients comprise primarily the ‘metastable proteome’, a set of structurally dynamic proteins that need constant chaperone surveillance. Importantly, acute accumulation of misfolded proteins under stress conditions (such as heat stress) causes rapid induction of PN components to reestablish proteome balance. However, this fails to occur when aberrant protein species are produced chronically, as in disease or during aging (Fig. 2C) [7].

HSPs are classified into families of differing molecular weights, which is reflected by their nomenclature, e.g. the 70 kDa protein family is called HSP70. Proteins of a given family may fulfill various functions [5].

1.2 HSP70s

The ubiquitous HSP70s and their constitutive cognates (HSC70s) are highly conserved in evolution. HSP70s are present in mammalian cells as two different gene products that are closely related: a stress-inducible form, HSP70 (known as HSP72), and a constitutively expressed form, HSC70 (known as HSP73). HSP70s consist of two

domains, a highly conserved NH2-terminal ATPase domain with a molecular mass of 45 kDa and a COOH terminal domain of 25 kDa (Fig. 3). The polypeptide-binding site is located in the 18-kDa of the COOH-terminal adjacent to the ATPase domain. The ATP-bound form of HSP70 binds and releases peptide rapidly, whereas the ADP form binds peptide slowly and in a more stable complex. The C-terminal peptide-binding domain of HSC70 binds to heat shock factor-1 (HSF-1) and the activation of HSF-1 is suppressed under normal conditions. In a previous study, it was reported that HSC70 and HSP70 specifically bind to a GGA-affinity matrix. When concentration of the GGA is increased in the cell, GGA preferentially binds to the C-terminal of HSC70 and dissociates HSF-1. The released HSF-1 is phosphorylated and activated, acquiring the ability to bind to a heat shock element (HSE) in the promoter of the heat-inducible HSP70 gene and resulting in induction of HSP70 expression.

Two groups of HSP proteins with a molecular weight of 70kDa are distinguished: HSP72, the concentration of which markedly increases in stress situations, and HSP73, which manifests stable expression regardless of the conditions [8-10]. The decisive majority of studies on the kinetics of expression involving proteins of the HSP70 family thus pertain to HSP72. The specific transcription factor HSF1 is responsible for the expression of HSP proteins. In stress situations it activates the gene coding for HSP70 proteins. The presence of HSP70 proteins in augmented amounts may be a factor that inhibits the development of the inflammatory process in colorectal mucosa. This conclusion can be drawn from an experiment conducted on mice devoid of the genes that code for macrophage migration inhibitory factor.

In the ATP-dependent mechanism of chaperone action, *de novo* folding and protein refolding is promoted through kinetic partitioning (Fig. 4). Chaperone binding (or rebinding) to hydrophobic regions of a non-native protein transiently blocks

aggregation; ATP-triggered release allows folding to proceed. Importantly, although the HSP70s and the chaperonins both operate by this basic mechanism, they differ fundamentally in that the former (like all other ATP-dependent chaperones) release the substrate protein for folding into bulk solution, whereas the cylindrical chaperonins allow the folding of single protein molecules enclosed in a cage. The two systems act sequentially, whereby HSP70 interacts upstream with nascent and newly synthesized polypeptides and the chaperonins function downstream in the final folding of those proteins that fail to reach native state by cycling on HSP70 alone (Fig. 4). In the following sections, we will use the HSP70, chaperonin and HSP90 models to illustrate the basic mechanisms of the major cytosolic protein-folding machines. Client specific chaperones that function downstream of folding in mediating the assembly of oligomeric complexes are not discussed [6].

It is suspected that HSP70 expression is stimulated by the cells of the immune system. In an experiment conducted on mice genetically deprived of lymphocytes T and B, HSC73 expression was the same as in mice with the unmodified genome; expression of HSP70, in turn, was significantly lower in the mice devoid of the lymphocytes. Lymphocytes probably exert the detected effect through the production of cytokines, and interleukin-2 (IL-2) in particular. HSP protein induction was found to develop under the influence of other cytokines (IL-10, IL-11, IL-1β, TNF-α), but in this case it involved mainly the HSP25 family, with no effect on HSP72 and HSC73 [11, 12]. A reciprocal relation also exists between mediators of inflammatory conditions and HSP70. In a pharmacologically induced model of colorectal inflammation, in mice with augmented HSP70 expression a significantly lower expression was observed of pro-inflammatory cytokines, such as TNF-α, IL-6, IL-1β as well as lower macrophage activity, as compared to the control group. At the same time, the course of the morbid

process was much milder in the mice with augmented HSP70 expression [13]. HSP70 proteins also manifest an ability to stimulate the production of IL-10, which has been found to exert an anti-inflammatory effect in an experimental model of bacterial infection with Listeria monocytogenes and in experimentally induced arthritis [1].

1.3 HSP70 in *H. pylori*-induced gastritis

Helicobacter pylori (*H. pylori*) infection leads to significant inflammation in the gastric mucosa, which is closely associated with development of gastric cancer. *H. pylori* is recognized as an important cause of gastritis, peptic ulcer disease, and also associated with mucosa-associated lymphoid tissue (MALT) lymphoma and gastric cancer. *H. pylori* have high urease activity that results in the production of ammonia and elicits oxidative burst of neutrophils. *H. pylori*-activated neutrophils reduce O_2 to superoxide (O_2-), and dismutation of O_2- yields more reactive radical of hydrogen peroxide (H_2O_2). Myeloperoxidase-catalyzed oxidation of chloride by H_2O_2 yields hypochlorous acid (HOCl), and the reaction of HOCl with ammonium (NH_4^+) yields monochloramine (NH_2Cl), which is a stable, lipophilic oxidizing agent that readily penetrates the membranes of target cells and exhibits a greater cytotoxicity in gastric mucosal cells than did H_2O_2 or HOCl. In animal and human studies, several investigators have reported that NH2Cl causes the gastric mucosal injury *in vivo* and *in vitro*. Since *H. pylori*-associated inflammation is characterized by severe infiltration of neutrophils and mononuclear cells in the gastric mucosa, accumulation and activation of these inflammatory cells is related to the robust productions of inflammatory cytokines and resultant reactive oxygen free radicals.

Recent studies have demonstrated that mucosa levels of IL-1β, IL-6, IL-8 and TNF-α were significantly higher in *H. pylori* positive patients [14, 15]. In addition to these

damaging conditions, after sustained infection of H. pylori, the cancellation of HSP70 might be the prominent event leading to perpetuation of gastric inflammation and epithelial cell damages. As for plausible explanation of cancellation of HSP70 related to *H. pylori* infection, the inhibition of the activation of HSF or decrease in the formation of HSF-HSE complex might be possible. Thus, since deregulation of HSP70 might be the prime cause of *H. pylori*-associated mucosal damage, the induction of HSP70 may constitute a novel therapeutic approach for the prevention and treatment of this condition.

1.4 HSP70 in stress-induced gastritis

GGA, a therapeutic agent for gastric ulcer and gastritis known as HSP70 inducer, pretreated gastric cells preserved HSP70 in spite of *H. pylori* infection. HSP induction irrespective of modality, preserved HSPs resistance to invoking levels of iNOS or COX-2, major damaging factors after *H. pylori* infection. Stress induced mucosal damages can be lessened through the strategy to preserve HSPs even under the augmented exaggerated harsh attack of *H. pylori.*

1.5 *H. pylori* infection and treatment today

The microaerophilic gram-negative bacterium *Helicobacter pylori* can colonize the human stomach. It survives in the stomach by neutralizing gastric acid with ammonium ion, which is produced from urea by the action of *H. pylori* urease. The bacterium adheres in gastric epithelial cells via adhesions, and grows in the mucus layer. *H. pylori* is an important etiological agent of gastroduodenal diseases, such as gastritis, gastric and duodenal ulcers, gastric cancer, and mucosa-associated lymphoid tissue (MALT) lymphoma. During prolonged chronic infection, the major cause of the symptoms is the

resultant inflammatory reaction. *H. pylori*-induced diseases are primarily treated with eradication therapy by antibiotics. The first-line eradication regiment is a three-drug combination therapy using a proton pump inhibitor (such as lansoprazole, omeprazole, rabeprazole, or esomeprazole), amoxicillin, and clarithromycin. Recently, failures of this treatment have increased, because of the appearance of antibiotic-resistant (especially clarithromycin) *H. pylori*. Metronidazole and sitafloxacin, instead of clarithromycin, are recommended for second and third line therapies in Japan.

H. pylori cells in biopsy specimens from patients' stomachs showed elongated rod-shaped or coccoid morphologies in variable proportions. The predominance of rods in exponentially growing *in-vitro* cultures suggests that this form represents proliferating cells, namely the vegetative form. On the other hand, the coccoid form is recognized as a viable-but-not-culturable state, which is resistant to various environmental stresses, such as starvation. The coccoid form could contaminate environments such as drinking water, thereby leading to oral transmission.

1.6 GGA

Geranylgeranylacetone (6,10,14,18-tetramethyl-5,9,13,17-nonadecatetraen-2-one; GGA, Eisai, Japan) is an anti-peptic ulcer drug developed and approved in Japan in 1984. GGA is shown to suppress *H. pylori*-induced tissue and cell injury and inflammatory reaction, therefore it is expected to show beneficial effects on *H. pylori*-infected tissues. One of pharmacological actions of GGA is induction of molecular chaperone 70-kDa heat shock protein (HSP70) in mammals. The induced HSP70 protects the gastrointestinal tract from cell damage induced by various stresses, such as reactive oxygen, ethanol and non-steroidal anti-inflammatory drugs (NSAIDs). In addition, mammalian HSP70 induced by GGA has been reported to be cytoprotective

in a number of pathological lesions other than the gastrointestinal tract, including heart ischemia, hepatectomy, cerebral infarction, and colitis.

In this study, the effect of GGA on *H. pylori*, a causative factor of gastrointestinal diseases, was examined. In the previous study of GGA effects on *H. pylori*, it was reported that GGA bounds to *H. pylori* HSP70 (product of DnaK gene) with 26-times higher affinity than to human HSP70, and induces large conformational changes as observed from surface plasmon resonance and circular dichroism. Binding of GGA suppressed the activity of the *H. pylori* chaperone [16, 17]. GGA also altered several characteristics of *H. pylori* cells. GGA-treated cells elicited enhanced interleukin-8 production by gastric cell lines and potentiated susceptibility to complement, as compared to untreated cells.

GGA also caused morphological alteration in *H. pylori* as reflected in fewer coccoid-like cells, suggesting that GGA converts *H. pylori* to an actively dividing, spiral state (vegetative form) from a non-growing, coccoid state. This morphological conversion of GGA resulted in accelerated growth of *H. pylori*. These results suggest a model in which GGA sensitizes *H. pylori* to antibiotic treatment by converting the cells to an actively growing state.

HSPs are highly conserved between mammals and bacteria, so it was anticipated that GGA could also bind to the HSP70 of *H. pylori* (product of the DnaK gene). It is important to establish whether GGA acts on both human and *H. pylori* cells. A previous report showed that GGA has antibacterial activity against *H. pylori*, but not *Campylobacter jejuni* [18]. In this study, the properties of binding of GGA to both *H. pylori* and human HSP70 were investigated, as well the effect of GGA on *H. pylori* cell.

Chaper II

Results

Chapter II

Results

2.1 Purification of human and *H. pylori* HSP70s

The sequence homology between human HSP70 and *H. pylori* DnaK was investigated. It has been shown that HSP70 is composed of two domains: ATPase and peptide-binding domain. The ATPase and peptide binding domains are located in the N-terminal and C-terminal halves of the protein respectively. There was 47% sequence identity between those two proteins, which was evenly distributed across the two halves (Fig. 5). There are some differences in the peptide-binding domains. After expression and purification, the human and *H. pylori* proteins were compared by SDS-PAGE (Fig. 6). The apparent molecular weight of the *H. pylori* protein (referred to henceforth as DnaK) was slightly larger. These purified proteins were used in the present study.

2.2 Affinity of GGA for HSP70 and DnaK

A sensorgram from surface plasmon resonance of the binding of GGA to HSP70 and DnaK is shown in Fig. 7. The kinetic parameters K_a, K_d, and K_D were estimated using BIACore evaluation software (BIAevaluation, version 3.0), fitting the binding curves to a simple bimolecular binding algorithm. Based on these results with immobilized HSP70 and soluble GGA, the apparent equilibrium dissociation constant (K_D) was 2.00×10^{-6} M. On the contrary, the K_D value of DnaK and GGA was calculated as 7.55×10^{-8} M. Thus, the affinity of GGA to the bacterial DnaK is about 26 times higher than that to mammalian HSP70.

2.3 Changes in HSP70 and DnaK conformation upon binding of GGA

It was investigated whether GGA may give rise to conformational change in HSP70 and DnaK using far UV Circular Dichroism (CD) spectra (Fig. 8). GGA induced changes in DnaK spectrum (Fig. 8A) that were consistent with decreased β-sheet and increased α-helix, β-turn (22.0 ± 1.4 to 24.0 ± 1.0), β-sheet (16.2 ± 2.3 to 9.4 ± 3.0* (*$p<0.05$), β-turn (25.2 ± 1.4 to 28.3 ± 1.6), and random structure (36.5 ± 0.9 to 38.3 ± 0.8). In contrast, GGA caused only slight conformational changes in HSP70 (Fig. 8B) α-helix (26.4 ± 3.9 to 27.0 ± 6.4), β-sheet (27.0 ± 0.7 to 24.4 ± 2.9), β-turn (26.1 ± 2.5 to 26.1 ± 5.2), and random structure (20.4 ± 1.7 to 22.4 ± 4.6). The conformational changes in HSP70 and DnaK in the presence or absence of GGA are summarized in Table 1.

2.4 Effect of GGA on chaperone activity of DnaK and HSC70

We compared the effect of GGA on the chaperone activities of DnaK and HSP70. Citrate synthase (CS) is very unstable to heat (see Fig. 9 for the thermal aggregation assay). Both DnaK (Fig. 9A) and HSP70 (fig. 9B) inhibited CS aggregation completely. GGA had only slight effect on chaperone activity of HSP70 (Fig. 9B). HSP 70 activity was reduced by only 15 % at 5 mM GGA; and reduced by 10 and 5% at 2.5 and 0.5 mM, respectively. In contrast, the chaperone activity of DnaK was inhibited almost completely at GGA 5mM (Fig. 9). These results are consistent with an influence of the drug on conformations of the two proteins.

2.5 Effect of GGA on growth and morphology of *H. pylori*

In broth culture medium, GGA accelerated the growth of *H. pylori* in a dose-dependent manner (Fig. 10). Microscopic observation of the cells from these cultures

revealed a mixture of Gram-negative rods and small spherical forms. A Gram stained micrograph of typical coccoid-form cells was shown in Fig. 10-D as a control. The coccoid-form cells were round and deeper pink than the rod-shaped cells. GGA caused a disappearance of coccoid-like form cells in a dose-dependent manner (Fig. 11). Therefore, GGA decreased the occurrence of the viable-but-not-culturable coccoid form, and increased highly dividing rod-shaped cells in these cultures of *H. pylori.*

2.6 Effect of GGA on serum sensitivity of *H. pylori*

The changes of cell morphology suggest that cell surface of *H. pylori* may be altered by GGA treatment. Therefore the effect of GGA treatment on serum sensitivity, namely antibody-independent complement-mediated killing, was examined. Normal rabbit serum was used as a source of complement. GGA-treated *H. pylori* cells were more rapidly killed by serum than the untreated cells (Fig. 12), which is consistent with the GGA-treated cells being more susceptible to complement.

2.7 Effect of GGA on induction of IL-8 gastric cancer cell lines by *H. pylori*

The effect of GGA pretreatment of *H. pylori* cells on their induction of IL-8 in gastric carcinoma cells lines; MKN28 and MKN45, was examined. IL-8 is the most important chemokine produced by epithelial cell lines for the inflammatory response induction and pathogenesis of *H. pylori*. GGA pretreatment decreased the ability of *H. pylori* to induce IL-8 in both cancer cell lines (Fig. 13).

Table I

Conformational changes in HSP70 and DnaK in the presence or absence of GGA

(%)	HSP70 -GGA	HSP70 + GGA	DnaK - GGA	DnaK + GGA
α-helix	26.4 ± 3.9	27.0 ± 6.4	22.0 ± 1.4	24.0 ± 1.0
β-sheet	27.0 ± 0.7	24.4 ± 2.9	16.2 ± 2.3	9.4 ± 3.0*
β-turn	26.1 ± 2.5	26.1 ± 5.2	25.2 ± 1.4	28.3 ± 1.6
random	20.4 ± 1.7	22.4 ± 4.6	36.5 ± 0.9	38.3 ± 0.8

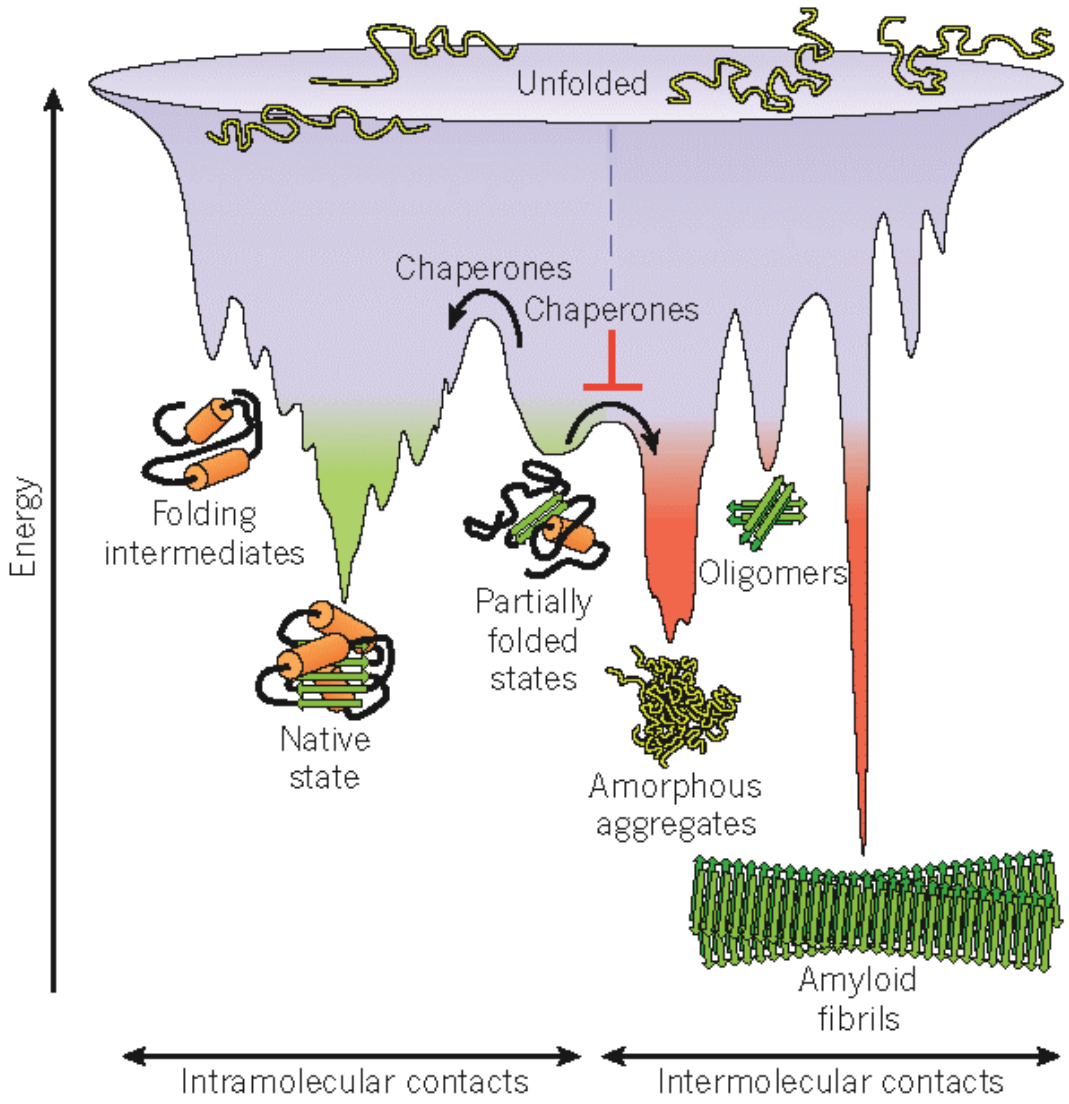

Figure 1 | Competing reactions of protein folding and aggregation. Scheme of the funnel-shaped free-energy surface that proteins explore as they move towards the native state (green) by forming intramolecular contacts. The ruggedness of the free-energy landscape results in the accumulation of kinetically trapped conformations that need to traverse free-energy barriers to reach a favourable downhill path. In vivo, these steps may be accelerated by chaperones. When several molecules fold simultaneously in the same compartment, the free-energy surface of folding may overlap with that of intermolecular aggregation, resulting in the formation of amorphous aggregates, toxic oligomers or ordered amyloid fibrils (red). Fibrillar aggregation typically occurs by nucleation-dependent polymerization. It may initiate from intermediates populated during de novo folding or after destabilization of the native state (partially folded states) and is normally prevented by molecular chaperones [6].

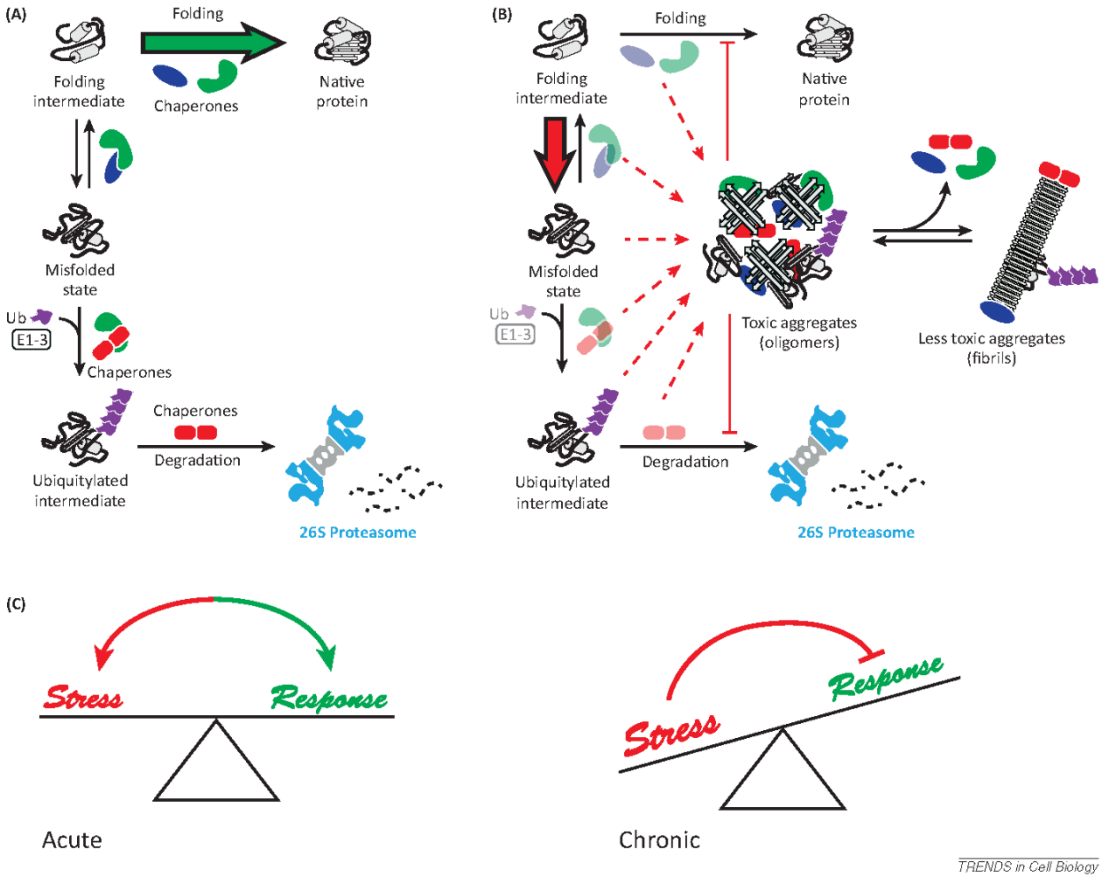

Figure 2. Mechanisms of proteostasis impairment. (A) Homeostasis. The capacity of the chaperone network is sufficient to correctly fold most newly synthesized proteins. The limited fraction of proteins that cannot be successfully folded on synthesis (∼5-10% of total) are degraded by the ubiquitin–proteasome system (UPS), a process that may contribute to the production of antigenic peptides. **(B)** Proteostasis network (PN) impairment by aggregate formation. Chaperone components are engaged and functionally depleted by soluble and insoluble protein aggregates (chaperone titration model). This prevents successful folding of endogenous chaperone clients and results in the accumulation of folding intermediates and misfolded states, which are ubiquitylated and directed toward proteasomal degradation. When the accumulation of misfolded proteins exceeds the capacity of the UPS, additional protein aggregates containing ubiquitylated and nonubiquitylated protein molecules form. These aggregates engage additional PN components, exacerbating PN impairment. Formation of insoluble inclusions may serve a protective role by binding fewer PN components. **(C)** Acute versus chronic stress. Eukaryotic cells contain multiple signaling mechanisms that respond to acute forms of conformational stress, such as the cytosolic heat-stress response (HSR) and the unfolded-protein response (UPR) of the ER. Activation of these pathways by the accumulation of misfolded proteins results in rapid induction of PN components, especially chaperones and degradation machinery. Simultaneously, synthesis of most other proteins is reduced, to free PN capacity for the removal of misfolded proteins. However, this cellular state is sustainable for a limited period only and if maintained for too long can result in apoptosis. Chronic stress, such as the constant production of protein aggregates during disease or aging, is thought to render cells stress refractory, thereby enhancing proteome imbalance [7].

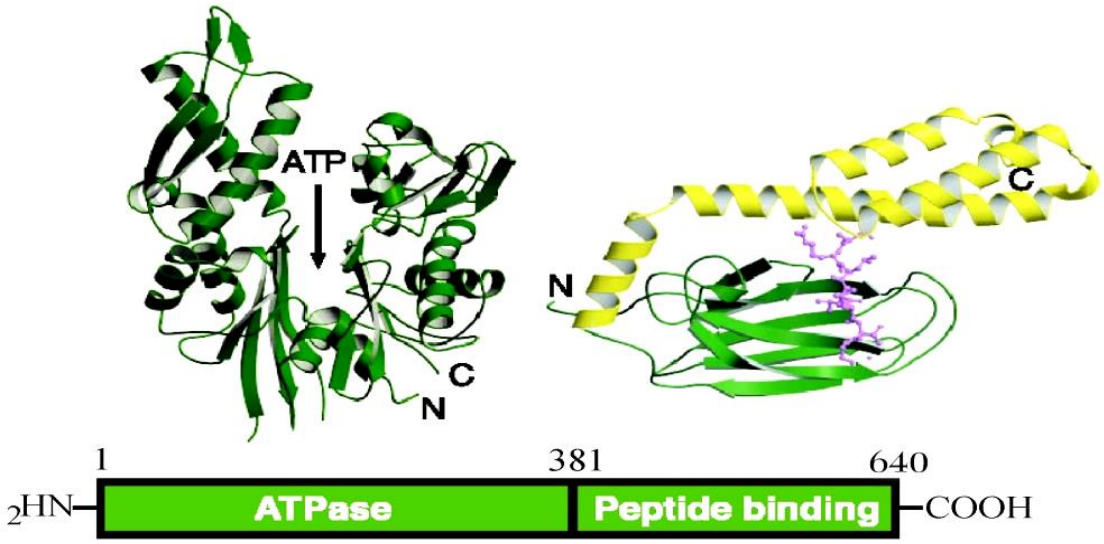

Figure 3. Domain structure of human HSP70. HSP70s consist of two domains, a highly conserved NH_2-terminal ATPase domain with a molecular mass of 45 kDa and a COOH terminal domain of 25 kDa**.**

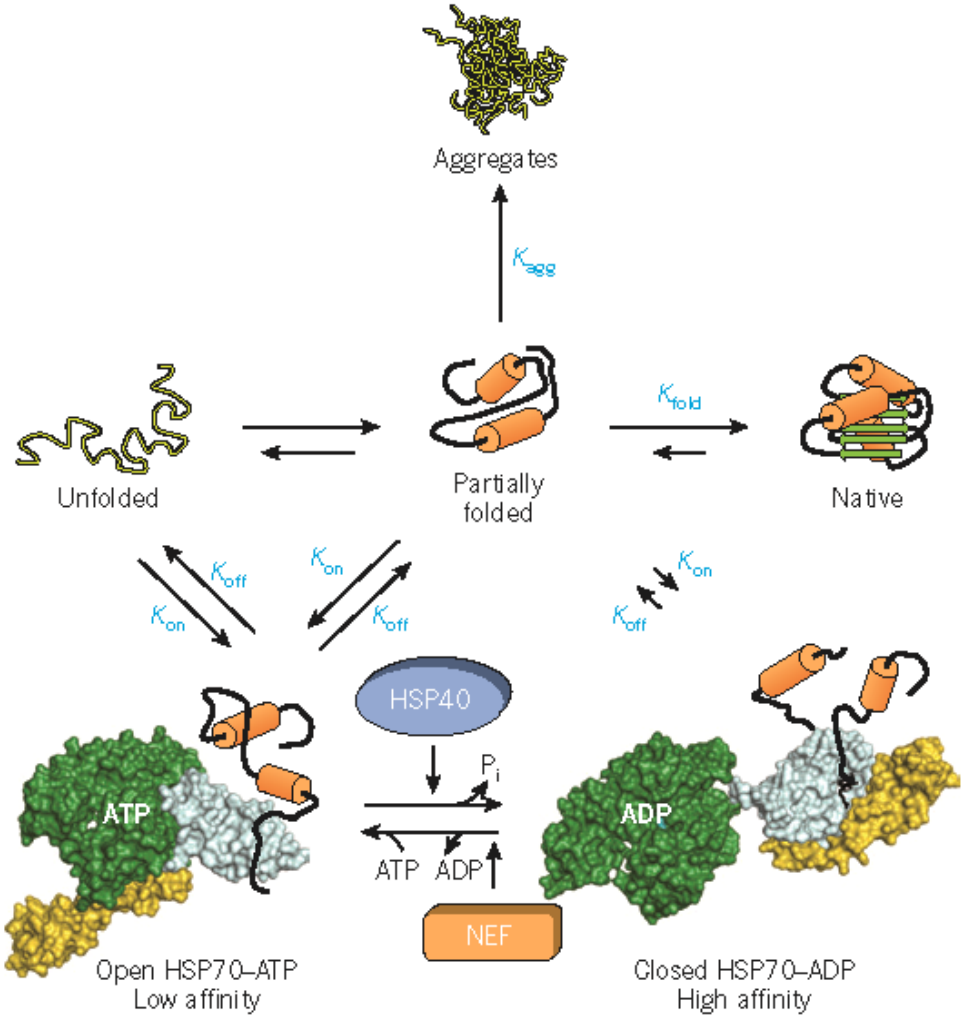

Figure 4 | The HSP70 chaperone cycle. HSP70 is switched between high- and low-affinity states for unfolded and partially folded protein by ATP binding and hydrolysis. Unfolded and partially folded substrate (nascent chain or stress-denatured protein), exposing hydrophobic peptide segments, is delivered to ATP-bound HSP70 (open; low substrate affinity with high on-rates and off-rates) by one of several HSP40 cofactors. The hydrolysis of ATP, which is accelerated by HSP40, results in closing of the α-helical lid of the peptide-binding domain (yellow) and tight binding of substrate by HSP70 (closed; high affinity with low on-rates and off-rates). Dissociation of ADP catalysed by one of several nucleotide-exchange factors (NEFs) is required for recycling. Opening of the α-helical lid, induced by ATP binding, results in substrate release. Folding is promoted and aggregation is prevented when both the folding rate constant (K_{fold}) is greater than the association constant (K_{on}) for chaperone binding (or rebinding) of partially folded states, and K_{on} is greater than intermolecular association by the higher-order aggregation rate constant K_{agg} ($K_{fold} > K_{on} > K_{agg}$) (kinetic partitioning). For proteins that populate misfolded states, *K*on may be greater than K_{fold} ($K_{fold} \leq K_{on} > K_{agg}$). These proteins are stabilized by HSP70 in a non-aggregated state, but require transfer into the chaperonin cage for folding. After conformational stress, K_{agg} may become faster than K_{on}, and aggregation occurs ($K_{agg} > K_{on} \geq K_{fold}$), unless chaperone expression is induced via the stress-response pathway. Structures in this figure relate to Protein Data Bank (PDB) accession codes 1DKG, 1DKZ, 2KHO and 2QXL. Pi, inorganic phosphate [6].

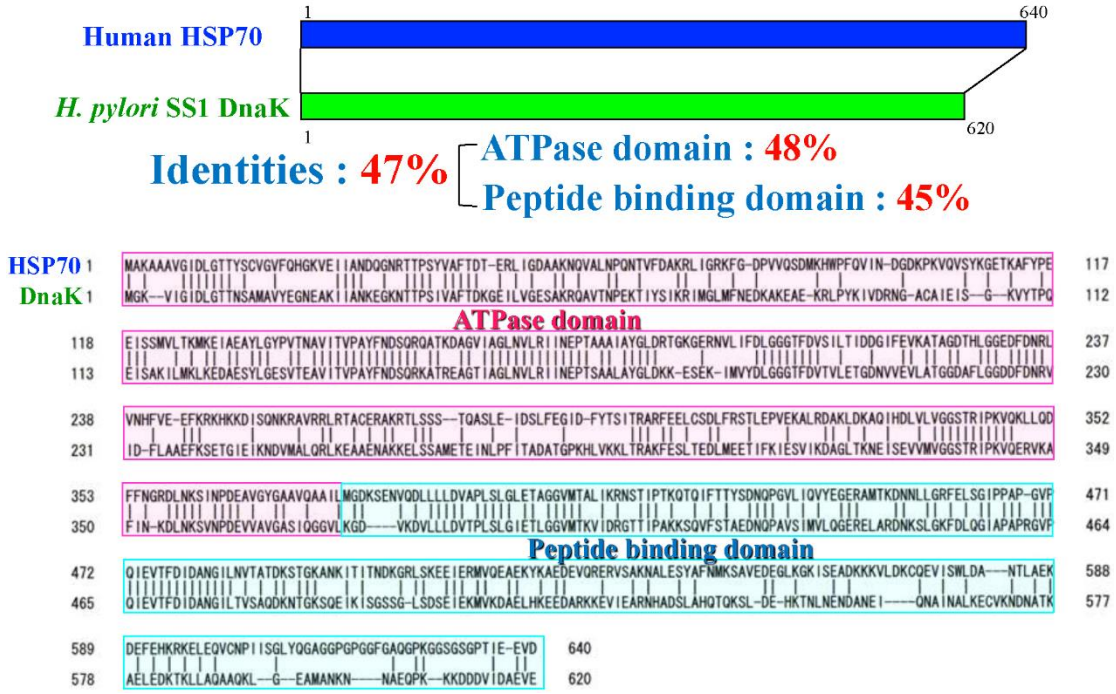

Figure 5. Sequence homology between human HSP70 and *H. Pylori* SS1 DnaK (HSP70 homologue). There was 47% homology between HSP70 and DnaK. The ATPase- and peptide binding domain of homology was 48- and 45%, respectively.

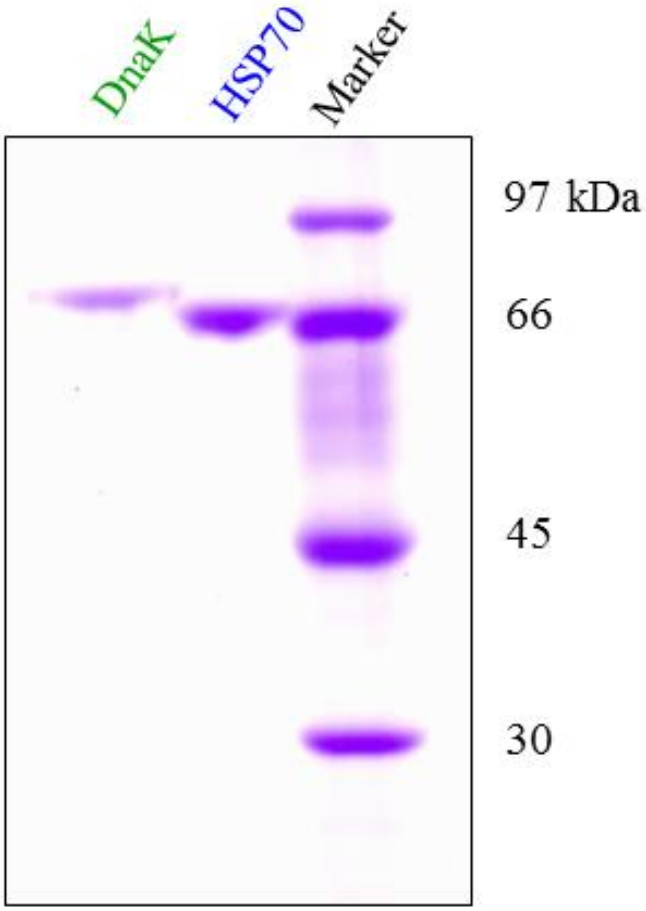

Figure 6. Purified DnaK and HSP70. DnaK and HSP70 were purified as described under "Materials and Methods" and the purity was analyzed by SDS-PAGE (9% gels).

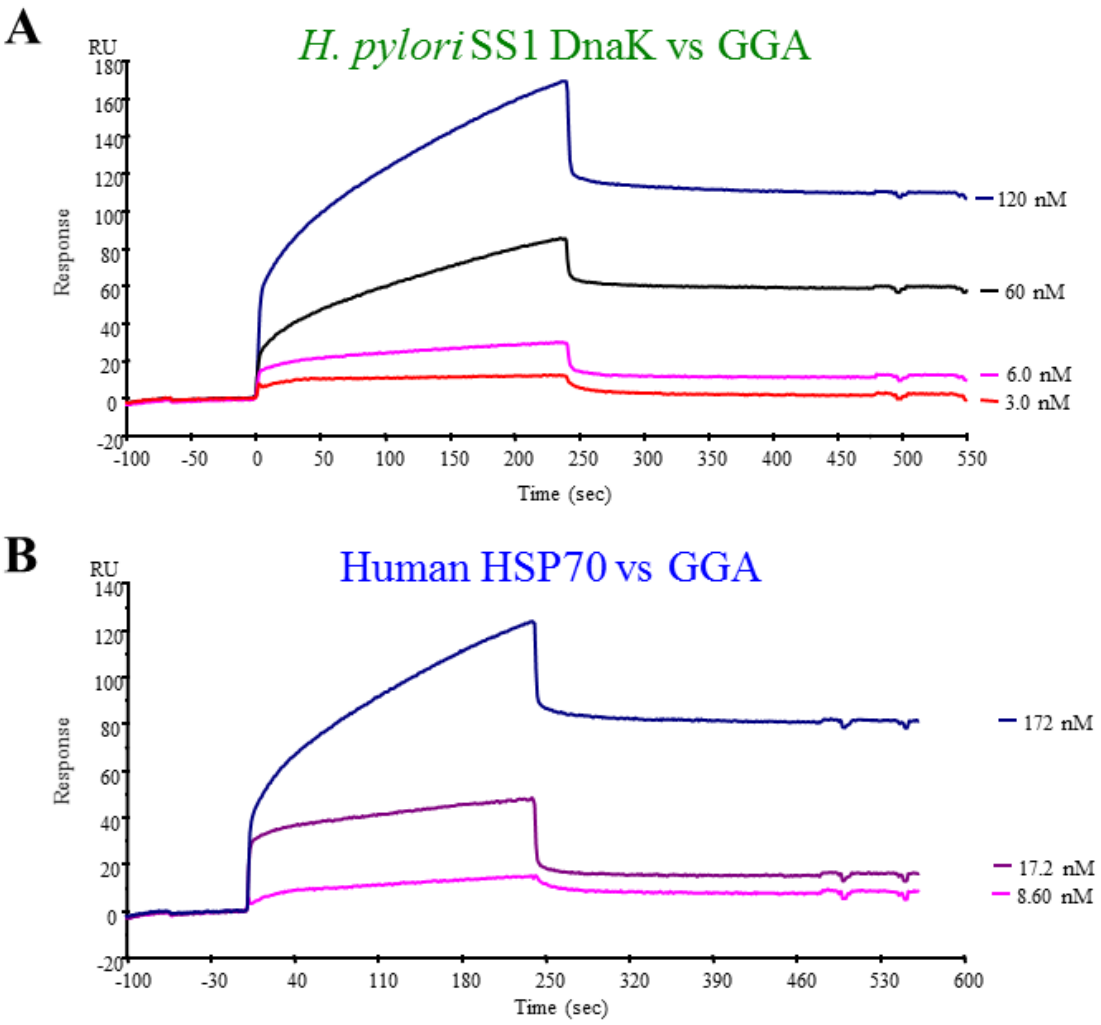

Figure 7. Surface plasmon resonance analysis of the interaction between HSP70 or DnaK and GGA. A sensorgram for the binding of DnaK (**A**) or HSP70 (**B**) to GGA is shown. Different concentrations of GGA were injected as described under "Materials and Methods". RU, resonance units.

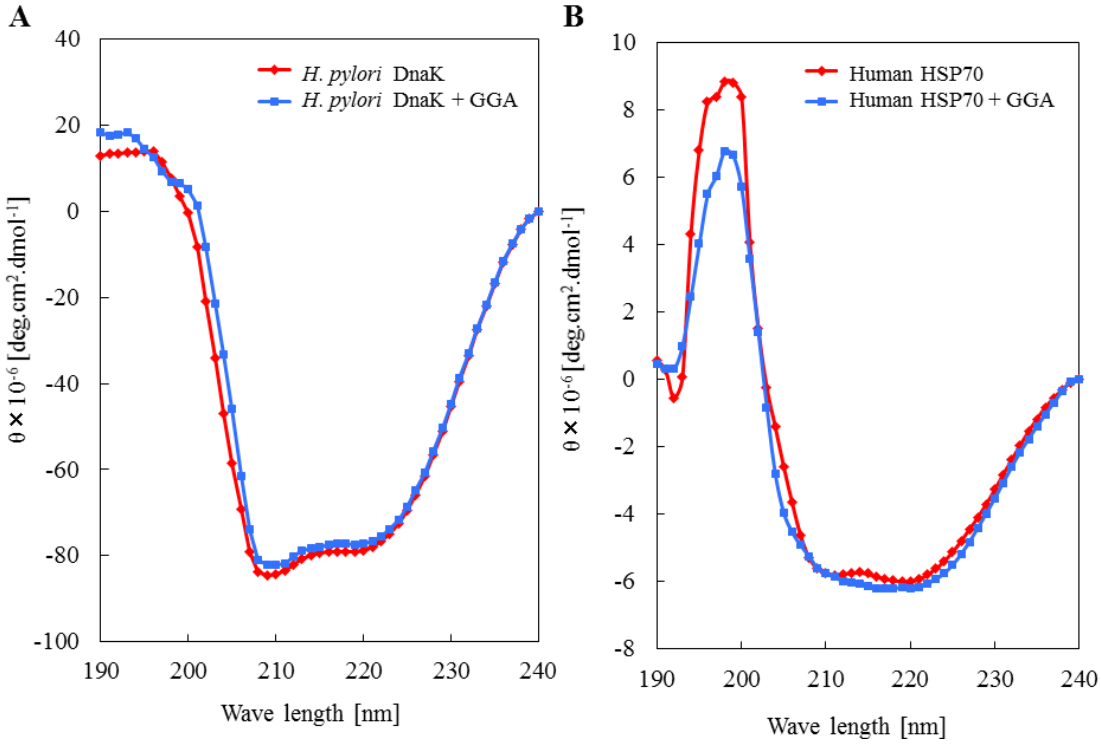

Figure 8. Effect of GGA on the conformational changes of DnaK and HSP70. A, the CD spectrum of DnaK was measured in the absence (closed red diamond) or presence (closed blue square) of GGA as described under "Materials and Methods" denotes the mean residue ellipticity. **B**, the CD spectrum of HSP70 was measured in the absence (closed red diamond) or presence (closed blue square) of GGA as described under "Materials and Methods" the mean residue ellipticity.

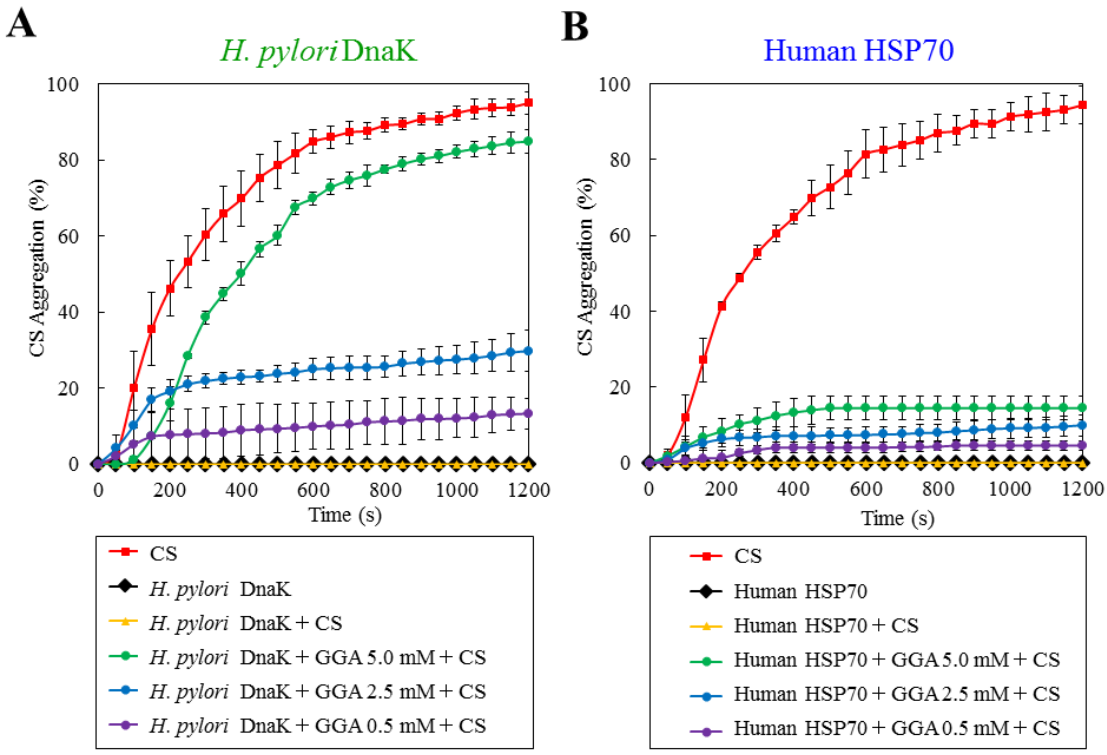

Figure 9. Effect of GGA on the chaperone activity of DnaK and HSP70. A, time course of 50 μM DnaK (closed black diamond), 0.5 M citrate synthase aggregation in buffer (closed red square), buffer containing 50 μM DnaK (closed yellow triangle), buffer containing 50 μM DnaK and 0.5 mM GGA (closed purple circle), buffer containing 50 μM DnaK and 2.5 mM GGA (closed blue circle), and buffer containing 50 μM DnaK and 5.0 mM GGA (closed green circle). **B**, time course of 50 μM HSP70 (closed black diamond), 0.5 M citrate synthase aggregation in buffer (closed red square), buffer containing 50 μM HSP70 (closed yellow triangle), buffer containing 50 μM HSP70 and 0.5 mM GGA (closed purple circle), buffer containing 50 μM HSP70 and 2.5 mM GGA (closed blue circle), and buffer containing 50 μM HSP70 and 5.0 mM GGA (closed green circle).

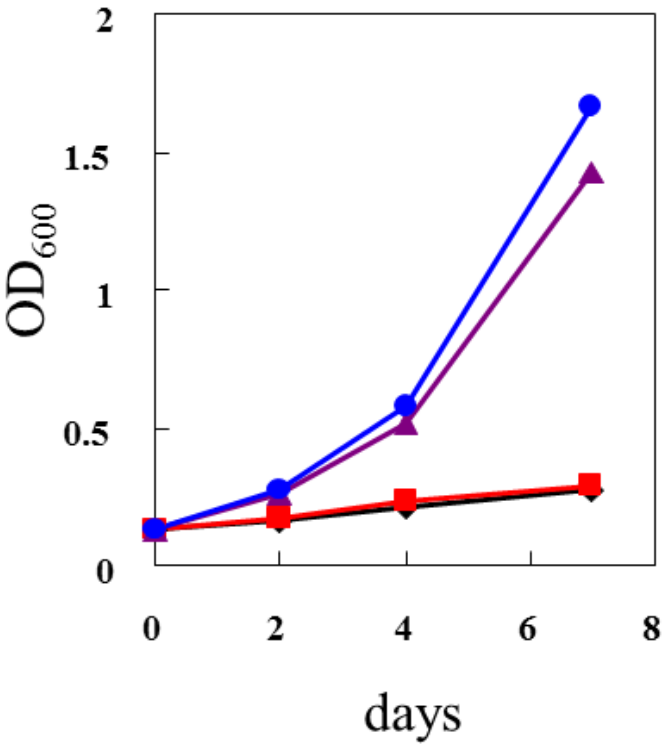

Figure 10. Effect of GGA on *H. pylori* cell growth. GGA was added to *H. pylori* SS1 culture in BHI-FBS broth at 37 °C under microaerophilic condition at a concentration of 0 (closed black diamond), 0.2 (closed red square), 1 (closed purple triangle), or 5 (closed blue circle) mM. The cells were cultured, and turbidity (determined by A_{600}) was measured.

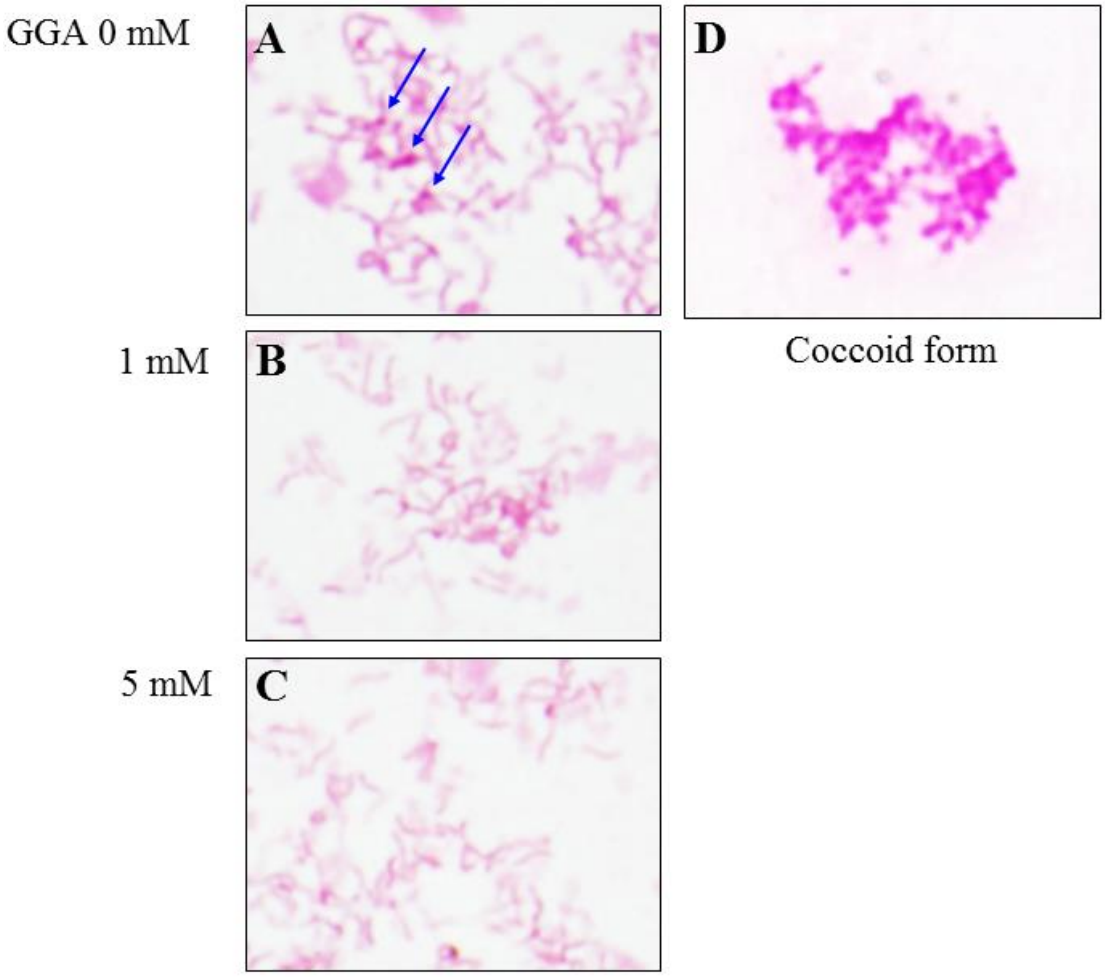

Figure 11. Effect of GGA on *H. pylori* cell morphology. *H. pylori* SS1 was cultured in BHI-FBS broth at 37 ^{o}C under microaerophilic condition in the absence or presence of GGA at a concentration of 0 (**A**), 1 (**B**), and 5 mM (**C**). Bacterial smear was stained by Gram staining. Coccoid form cells (**D**) were prepared by cultivation under anaerobic condition. Arrows in (**A**) indicate coccoid-like cells.

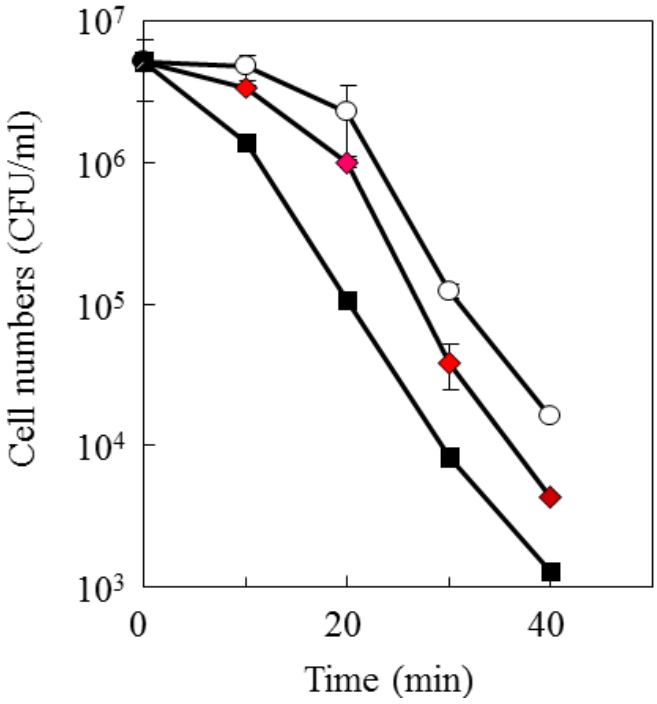

Figure 12. Effect of GGA on serum sensitivity of *H. pylori* cells. *H. pylori* SS1 was precultured in the absence or presence of GGA at a concentration of 0 (open circle), 1 (closed red diamond), and 5 (closed black square) mM. The resulting cells were treated with 50% normal rabbit serum as a source of complement. After incubation at various times, the suspension was diluted appropriately and plated on sheep blood agar plates. After 72 h culture, the colonies were counted. Each experiment was performed in quadruplicate.

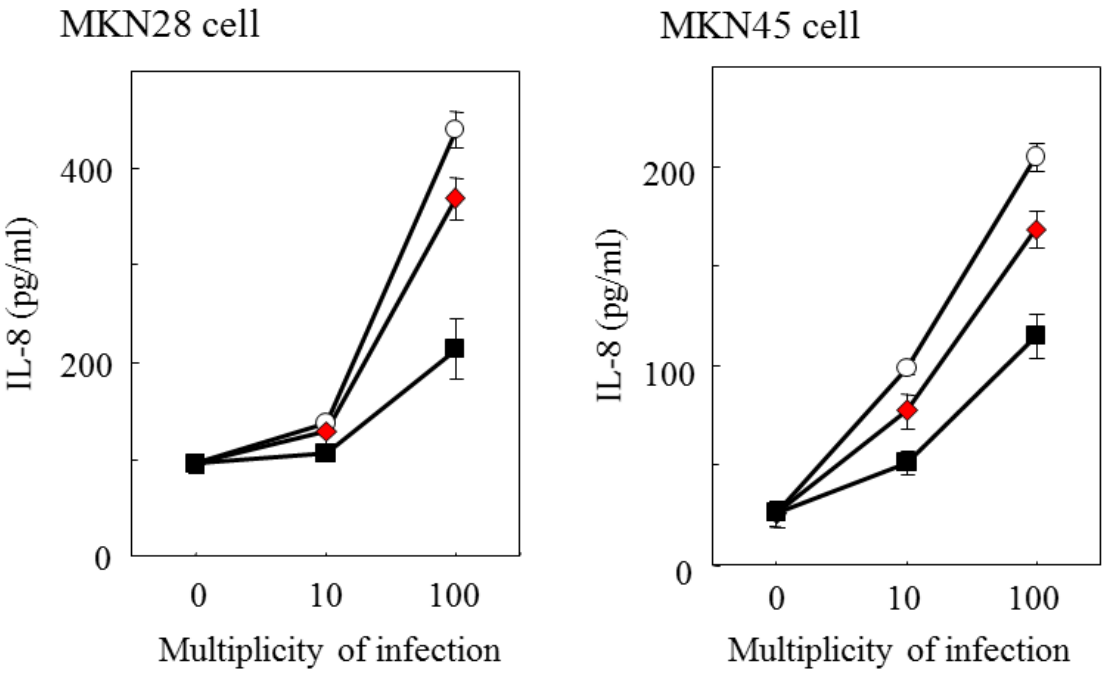

Figure 13. Effect of GGA on IL-8 production induced by *H. pylori* live cells in gastric carcinoma cell line MKN28 and MKN45. *H. pylori* SS1 was precultured in the absence or presence of GGA at a concentration of 0 (open circle), 1 (closed red diamond), and 5 (closed black square) mM. The resulting cells were inoculated to MKN28 cells or MKN45 cells at MOI 10 or 100. After 24 h incubation, IL-8 in the culture supernatant was measured by ELISA. Each experiment was performed in triplicate.

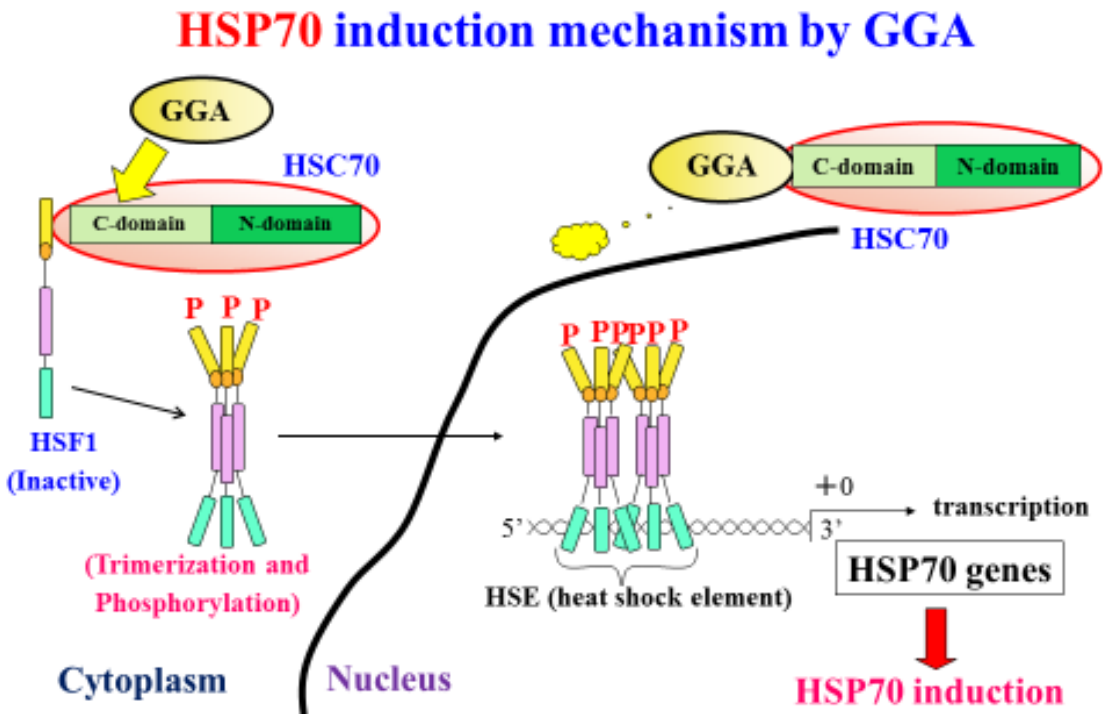

Figure 14. Human HSP70 induction mechanism by GGA

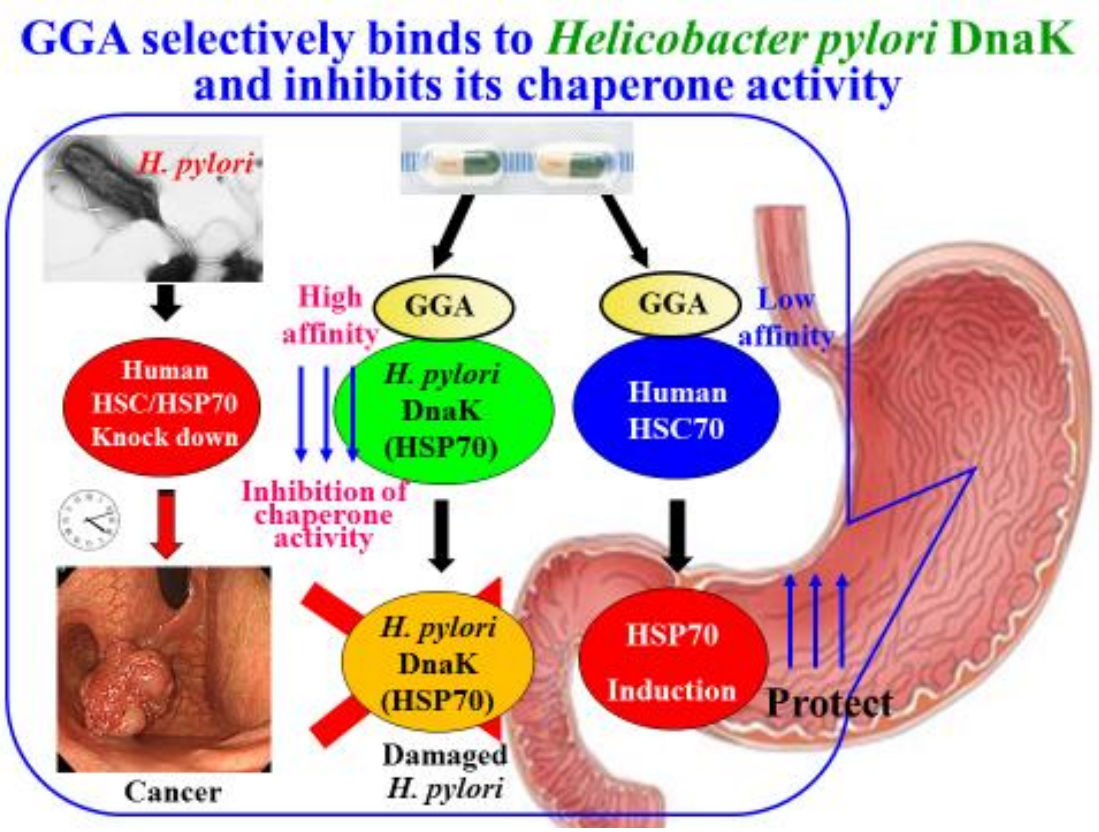

Figure 15. GGA selectively binds to Helicobacter pylori DnaK and inhibits its chaperone activity

Chaper III

Discussion

Discussion

GGA is a gastromucoprotective drug with a low incidence of side effects. It is employed to treat gastritis/gastric ulcers in Japan and other Asian countries. GGA is commonly employed as an HSP inducing agent. HSP promotes protein folding/membrane passage and protects cells against various types of stressors including infection and inflammation. Organs/cells in which HSP has been induced show a potent activity to resist toxic substances. There are many reports of *in vivo* experiments, including a human clinical study, that GGA induces HSPs responsible for cell protection, for example, inhibiting NSAID-related acute gastric/small intestinal mucosal injury.

The previous study reported that mammalian HSP70/HSC70 was a GGA-specific binding protein and proposed induction mechanism of HSP70 by GGA. HSPs are highly conserved proteins among organisms, including prokaryote and eukaryote. The sequence homology between human HSP70 and H. pylori DnaK is 47%. Therefore, it was anticipated in this study that GGA would bind to *H. pylori* DnaK. In this study, this binding was investigated and the influence of GGA on *H. pylori* viable cells was discovered. GGA indeed bound to *H. pylori* DnaK with higher affinity than to human HSP70. The same concentration of GGA selectively affected the conformation and chaperone activity of *H. pylori* DnaK compared to those of human HSP70. There are some differences in amino acid sequences of the peptide-binding domain of human HSP70 and *H. pylori* DnaK. The sequence differences could result in different affinities for GGA.

GGA shares cell-protective effects, especially in gastric mucosa cells. There are a few reports that GGA protects from *H. pylori*-induced gastric injury. For example, GGA reduced *H. pylori*-induced gastric mucosa injury in an experiment using a rat *in vivo* mode [19]. GGA accentuated growth suppression of human umbilical vein epithelial cells induced by *H. pylori* cell extract, and the authors speculate that GGA could recover host angiogenesis, which is important for the healing of gastric ulcer [20]. The results of that study lead to a conclusion that GGA is a promising agent, effective against *H. pylori*-induces pathologies. Effects of GGA on *H. pylori* cells and *H. pylori*-induced immune responses have been found in several reports and were observed in present study. Ishii reported that GGA showed antibacterial activity to *H. pylori*, however, it highly depended on supplements to media [21]. The antibacterial activity was observed on Brucella agar containing albumin, charcoal, or egg yolk emulsion, but it was not observed on the agar containing horse defibrinated blood or β-cyclodextrin. Conversely, our present study indicated that GGA accelerated growth rate of *H. pylori* in BHI-FBS broth (Fig. 10) and Brucella broth containing FBS. An explanation of the growth enhancement was that GGA converted *H. pylori* to vegetative phase from the coccoid form (Fig. 11). The coccoid form of *H. pylori* is recognized as a viable-but-not-culturable state that is more resistant to environmental stresses than the vegetative state with active proliferation. Treatment with antibiotics, including β-lactams, such as amoxicillin, causes conversion of *H. pylori* to the coccoid form [22, 23]. Generally, antibiotics are effective on actively proliferating cells and, in fact, the coccoid form of *H. pylori* is less susceptible to antibiotic treatment [24, 25]. This incomplete eradication could explain relapse of *H. pylori*-induced gastric disorder after the antibiotics treatment [26]. GGA is expected to promote eradication of *H. pylori* through conversion to the vegetative form.

H. pylori is susceptible to antibody-independent complement killing [27]. Serum sensitivity of *H. pylori* was also observed in this study. Furthermore, GGA-treated cells were found to be more susceptible to complement killing. It seems that the morphological change from coccoid to vegetative form reflects an alteration of cell surface properties, resulting in greater sensitivity to complement killing.

Effects of GGA on a *H. pylori* cell-induced inflammatory response, IL-8 production, have been reported [28, 29]. In these reports, live *H. pylori* cells and GGA were simultaneously incubated with human gastric carcinoma cell lines, such as KATOIII and MKN28. It is unclear, however, if GGA affected the gastric or *H. pylori* cells. In this study, experiment was conducted under conditions in which *H. pylori* cells were pre-treated with GGA and then co-cultured with human gastric cells under GGA-free conditions. Therefore, it has been suggested that suppression of IL-8 induction occurred by direct action of GGA on the bacteria. Induction of NF-κB activation and proinflammatory cytokine production has been shown to be mediated by the type IV secretion system of bacterial cells [30-32]. The type IV secretion system consists of proteins encoded by genes located on cag pathogenicity islands [33, 34]. GGA could suppress expression or function of this system. Poursina *et al.* reported that *cagE* mRNA, which encodes a key factor of type IV secretion system CagE, was expressed in coccoid cells, however, the expression levels in coccoid cells were lower than in the spiral form cells [34]. The issue needs to be clarified in the future study.

In conclusion, GGA acts on both human cells and *H. pylori* cells for protection from gastric disorder. For human cells, HSP70 induced GGA protects the gastric cells from injury induced by *H. pylori* (Fig. 14). For the *H. pylori* cells, GGA causes inhibition of

DnaK function, increase of complement susceptibility, suppression of IL-8 induction, and conversion to vegetative form from coccoid form. The sum of these actions on *H. pylori* should have a positive effect on the symptoms caused by the *H. pylori* infection (Fig. 15). Of greatest interest, the conversion to the vegetative form should increase the susceptibility of *H. pylori* to many antibiotics.

Chaper IV

Materials and Methods

Materials and Methods

Materials

GGA was obtained from Eisai (Tokyo, Japan). Human Hsp70 cDNA (kindly provided from Dr. Richard Morimoto, Northwestern University) was used in this study. Human HSP70 cDNA was amplified by PCR (iCycler BioRad) using HSP 70-specific primer containing the restriction enzyme site which forward primer is encoding Xba I site'- CTCGAGATGGGAAAAGTTATTGGAATTGAT-3'and reverse primer is encoding Xba I site 5'-TCYAGAGATTAAAACCGCTCGCTTGA-3' from *H. pylori* genomic DNA. The product obtained by PCR was inserted into Xho I/Xba I sites of the pCold I vector (TaKaRa Bio, Japan). The pCold I - *H.pylori* Dna K constructs were confirmed by DNA sequencing (PRISM 3100, ABI).

The pCold I - *H.pylori* DnaK was expressed in *Eschericha coli* BL21 (Promega). The cells were grown in the LB BROTH medium (Invitrogen) containing 100 μg/mL ampicillin until OD_{600} reached 0.4~0.5 at 37°C. The culture medium was left standing for 30 min to 15°C. The cells were added to 1 mM IPTG (Nacalai Tesque) to induce protein of interest, and incubated 24 hours at 15°C. The cells were sonicated, and centrifuged at 20,000 × g for 15 min at 4°C, and the supernatants were collected. The supernatants were mixed in equal amount of Ni column apply buffer (40 MM Imidazole in 10 mM Tris-HCl, pH 7.4), and applied onto Ni-NTA affinity column (GE Healthcare) equilibrated with Ni column equilibration buffer (20 mM Imidazole, 300 mM NaCl in 10 mM Tris-HCl, pH 7.4). After washing with Ni column wash buffer (50 mM Imidazole, 300 mM NaCl in 10 mM Tris-HCl, ph 7.4), proteins were eluted with a linear gradient of 0.1~0.5 M Imidazole in 0.3 M NaCl, 10 mM Tris-HCl, pH 7.4. *H. pylori* DnaK fractions were concentrated by ultrafiltration.

Surface Plasmon Resonance (SPR) assay

Surface plasmon resonance assay were performed as previously described [35]. All SPR measurements were performed on a BIAcore 2000 instrument (GE Helathcare) at 25°C, and 25 mM HEPES-KOH (pH 7.4) buffer containing 0.005% Tween 20, 5 mM $MgCl_2$, and 150 mM KCl was used as the running buffer at the flow rate of 10 μl/min. HSP70 or DnaK (1μM) were dissolved in 100 mM sodium acetate buffer (pH 4.0) and immobilized on CM5 sensor chips (GE Healthcare) by amino coupling. HSP70 (~15,000 RU) was immobilized on the chip, and GGA solutions (8.6, 17.2 and 172 nM) were loaded on the chip using running buffer. DnaK (~15,000 RU) was immobilized on the chip, and GGA solutions (3, 6, 60, and 120 nM) were loaded on the chip using running buffer. Regeneration of the sensor chip surface was achieved by 1-min pulse (1μl) of 0.5 M NaCl in running buffer. The dissociation constant (K_D) was obtained by non-linear curve fitting based on a steady-state affinity using BIAevaluation 3.0 software.

Far-UV Circular Dichroism (CD)

The CD measurements were performed by a J-720 spectropolarimeter (Jasco, Tokyo, Japan) as previously described [36]. The CD spectrum (190-240 nm) of HSP70 (1.1 μM) or DnaK (1.1 μM) in 50 mM HEPES-NaOH buffer (pH 7.4) in the presence or absence of GGA (11.0 μM) were recorded at 25°C using a cuvette with a 0.5-mm path length. The observed specific ellipticity after normalization against a blank was converted to the mean residue ellipticity [θ] (degrees cm^2 $dmol^{-1}$). The secondary structure of HSP70 or DnaK was calculated using an analytical program for secondary structure proteins (SSE-338W, Jasco, Tokyo, Japan).

Measurement of protein aggregation and chaperone function of HSPs

The thermal aggregation of citrate synthase (CS) (Roche Diagnostics, Manheim, Germany) was monitored at 50°C as previously described [16]. Briefly, the concentration of CS used was 0.25 μM in 50 mM Hepes buffer, pH 7.4, in presence or absence of the HSP70 (50μM) or DnaK (50μM), and in the presence of each HSP70 and GGA (0.5 to 5 mM). Light scattering CS was monitored for 20 min at an optical wavelength of 500 nm by Ultrospec 3000 UV-vis spectrophotometer (GE Healthcare) equipped with a temperature control unit using semi-micro-cuvettes (0.5 ml) with a path-length of 10 mm.

Bacterial cells and cultivation

H. pylori strain SS1 was donated by Dr. Adrian Lee (The University of New South Wales, Sydney, Australia). SS1 was cultured in brain heat infusion broth containing 5% (vol/vol) heat-inactivated fetal bovine serum (BHI-FBS) at 37°C in 5% CO_2, or Helicobacter agar plate (Nissui Pharmaceuticals, Tokyo, Japan) at 37°C under microareophic condition using AnaeroPack-MicroAero (Mitsubishi Gas Chemical, Tokyo, Japan). Cell growth was determined by turbidity (measured by absorbance at 600 nm). Cell numbers were determined by colony formation using tryptic soy agar plate containing 5% (v/v) sheep blood. Coccoid form cells were prepared according to Yamaguchi et al. [37]. Briefly, cells on *Helicobacter* agar plates cultured in microaerophic condition were subsequently cultured at 37°C for 7 d under anaerobic condition using AnaeroPack-Anaero (Mitsubishi Gas Chemical).

Gram staining

Gram staining was performed by Hucker's modified method using Gram Solutions (Wako Pure Chemical, Osaka, Japan).

Serum sensitivity assays

Cultured *H. pylori* SS1 cells were adjusted at a cell density of 10^7 cells/ml. GGA was added to the cell suspension at a concentration of 0, 1, or 5 mM, and then incubated for 48 h. The cells were collected by centrifugation, and then suspended with PBS at a cell density of approximately 10^7 cells/ml. The aliquots (200 μl) of the cell suspension were mixed with 200 μl of pooled normal rabbit serum (Cedarlane, Ontario, Canada), and then incubated for various times. After incubation, the treated cell suspension was immediately diluted with PBS at 10 to 10,000-fold and inoculated to tryptic soy agar containing 5% sheep blood. The plates were incubated for 72 h, and the resulting colonies were counted.

IL-8 inducing activity of *H. pylori* cells

The human gastric carcinoma cell lines MKN28 and MKN45 were obtained from the Japanese Collection of Research Biosources (JCRB, Ibaraki, Japan). MKN28 and MKN45 were routinely cultured in Dulbecco's modified minimum essential medium supplemented with 10% (vol/vol) heat-inactivated fetal bovine serum (DMEM-FBS). *H. pylori* cells were precultured in BHI-FBS for 72 h, and then GGA was added at a concentration of 0, 1, or 5 mM and further cultured for 48 h. The cells were collected by centrifugation and then washed with PBS twice. The treated cells were suspended with DMEM-FBS, and inoculated to MKN28 or MKN45 cells with approximately 70% confluency at a multiplicity of infection 10 or 100. After 24 h incubation, the amounts

of interleukin-8 (IL-8) in the culture supernatants were determined by enzyme-linked immunosorbent assay (ELISA) with an ELISA Development kit for human IL-8 (R&D Systems, Minneapolis, MN).

Acknowledgement

The author would like to thank Professor Hideaki Itoh of Department Life Science of Akita University for all his support, expertise and guidance throughout the study. And also thanks to all the students belonging to Prof. Itoh's laboratory for their kind assistance.

The author wishes to acknowledge contributions to this study made by Professors Shin-ichi Yokota and Soh Yamamoto of Sapporo Medical University. And also special thanks to Ms. Takako Ohtaki-Mizoguchi, whose study preceded and laid foundation to the present one.

References

[1] Borges TJ, Wieten L, van Herwijnen MJ, Broere F, van der Zee R, Bonorino C, van Eden W: The anti-inflammatory mechanisms of HSP70. *Front Immunol*, **3**, 95 (2012).

[2] Ritossa FA: A new puffing pattern induced by temperature shock and DNP in Drosophila. *Experientia*, **18**, 571-573 (1962).

[3] Tissières A, Mitchell HK, Tracy U: Protein synthesis in salivary glands of *Drosophila melanogaster*: relation to chromosome puffs. *J Mol Biol*, **84**, 389-398 (1974).

[4] Lindquist S: The heat-shock response. *Annu Rev Biochem*, **55**, 1151-1191 (1986) .

[5] Pockley AG: Heat shock proteins as regulators of the immune response. *Lancet*, **362**, 469–476 (2003).

[6] Hartl FU, Bracher A, Hayer-Hartl M.: Molecular chaperones in protein folding and proteostasis. *Nature*. **475**, 324-32 (2011) .

[7] Hipp MS, Park SH, Hartl FU.: Proteostasis impairment in protein-misfolding and aggregation diseases. *Trends Cell Biol.* **24**, 506-14 (2014).

[8] Otaka M, Odashima M, Watanabe S: Role of heat shock proteins (molecularchaperones) in intestinal mucosal protection. *Biochem Biophys Res Commun*, **348**, 1-5 (2006).

[9] Itoh H, Tashima Y: The stress (heat shock) proteins. *Int J Biochem*, **23**, 1185-191 (1991).

[10] Lindquist S: Varying patterns of protein synthesis in Drosophila during heat shock: implications for regulation. *Dev Biol*, **77**, 463-79 (1980).

[11] Kojima K, Musch MW, Ren H, Boone DL, Hendrickson BA, Ma A, Chang EB: Enteric flora and lymphocytederived cytokines determine expression of heat shock

proteins in mouse colonic epithelial cells. *Gastroenterology*, **124**, 1395-1407 (2003).

[12] Ropeleski MJ, Tang J, Walsh-Reitz MM, Musch MW, Chang EB: Interleukin-11-induced heat shock protein 25 confers intestinal epithelial-specific cytoprotection from oxidant stress. *Gastroenterology*, **124**, 1358-1368 (2003).

[13] Tanaka K, Namba T, Arai Y, Fujimoto M, Adachi H, Sobue G, Takeuchi K, Nakai A, Mizushima T: Genetic evidence for a protective role for heat shock factor 1 and heat shock protein 70 against colitis. *J Biol Chem*, **282**, 23240-23252 (2007).

[14] Crabtree JE, Peichl P, Wyatt J, Stachl U, Lindley IJ. Gastric interleukin-8 and IgA IL-8 autoantibodies in Helicobacer pylori infection. *Scand J Immunol*, **37**: 65-70 (1993).

[15] Yamaoka Y, Kita M, Kodama T, Sawai N, Kashima K, Imanishi J. Induction of various cytokines and development of severe mucosal inflammation by cagA gene positive Helicobacter pylori strains. *Gut.* **1**: 442-451 (1997).

[16] Otaka M, Yamamoto S, Ogasawara K, Takaoka Y, Noguchi S, Miyazaki T, Nakai A, Odashima M, Matsuhashi T, Watanabe S, Itoh H. The induction mechanism of the molecular chaperone HSP70 in the gastric mucosa by Geranylgeranylacetone (HSP-inducer). *Biochem Biophys Res Commun*. **353**:399-404. (2007)

[17] Grave E, Yokota S, Yamamoto S, Tamura A, Ohtaki-Mizoguchi T, Yokota K, Oguma K, Fujiwara K, Ogawa N, Okamoto T, Otaka M, Itoh H.: Geranylgeranylacetone selectively binds to the HSP70 of Helicobacter pylori and alters its coccoid morphology. *Sci Rep.* **5**:13738, DOI: 10.1038/srep13738 (2015).

[18]. Ishii, E.: Antibacterial activity of teprenone, a non water-soluble antiulcer agent, against *Helicobacter pylori*. *Zentralbl. Bakteriol*. **280**, 239-43 (1993).

[19] Freeman, B.C. Morimoto RI. The human cytosolic molecular chaperones hsp90, hsp70 (hsc70) and hdj-1 have distinct roles in recognition of a non-native protein and protein refolding. *EMBO J*. **15**, 2969-79 (1996).

[20] Tatsuta M, Iishi H, Baba M, Iseki K. Geranylgeranylacetone attenuates suppression by Helicobacter pylori extract of human umbilical vein epithelial cell growth. *Hepatogastroenterology*. **51**, 1558-60 (2004).

[21] Ishii, E. Antibacterial activity of teprenone, a non water-soluble antiulcer agent, against Helicobacter pylori. *Zentralbl. Bakteriol*. **280**, 239-43 (1993).

[22] DeLoney, C.R., & Schiller, N.L. Competition of various beta-lactam antibiotics for the major penicillin-binding proteins of *Helicobacter pylori*. antibacterial activity and effects on bacterial morphology. *Antimicrob. Agents. Chemother*. **43**, 2702-9 (1999).

[23] Berry V, Jennings K, Woodnutt G. Bactericidal and morphological effects of amoxicillin on Helicobacter pylori. *Antimicrob. Agents. Chemother*. **39**, 1859-61 (1995).

[24] Sörberg M, Hanberger H, Nilsson M, Björkman A, Nilsson LE. Risk of development of in vitro resistance to amoxicillin, clarithromycin, and metronidazole in Helicobacter pylori. *Antimicrob. Agents. Chemother*. **42**, 1222-8 (1998).

[25] Figura N, Moretti E, Vaglio L, Langone F, Vernillo R, Vindigni C, Giordano N. Factors modulating the outcome of treatment for the eradication of Helicobacter pylori infection. *New Microbiol*. **35**, 335-40 (2012).

[26] Brenciaglia MI, Fornara AM, Scaltrito MM, Dubini F. *Helicobacter pylori*: cultivability and antibiotic susceptibility of coccoid forms. *Int. J. Antimicrob. Agents*. **13**, 237-41 (2000).

[27] Gonzalez-Valencia G, Perez-Perez GI, Washburn RG, Blaser MJ. Susceptibility of Helicobacter pylori to the bactericidal activity of human serum. *Helicobacter*. **1**, 28-33 (1996).

[28] Miyake K, Tsukui T, Shinji Y, Shinoki K, Hiratsuka T, Nishigaki H, Futagami S, Wada K, Gudis K, Iwakiri K, Yamada N, Sakamoto C. et al. Teprenone, but not H2-receptor blocker or sucralfate, suppresses corpus Helicobacter pylori colonization and gastritis in humans: teprenone inhibition of *H. pylori*-induced interleukin-8 in MKN28 gastric epithelial cell lines. *Helicobacter*. **9**, 130-7 (2004).

[29] Yoshimura N, Suzuki Y, Saito Y. Suppression of Helicobacter pylori-induced interleukin-8 production in gastric cancer cell lines by an anti-ulcer drug, geranylgeranylacetone. *J. Gastroenterol. Hepatol*. **17**, 1153-60 (2002).

[30] Maeda S, Akanuma M, Mitsuno Y, Hirata Y, Ogura K, Yoshida H, Shiratori Y, Omata M. Distinct mechanism of Helicobacter pylori-mediated NF-kappa B activation between gastric cancer cells and monocytic cells. *J. Biol. Chem.* **276**, 44856-64 (2001).

[31] Shibata W, Hirata Y, Yoshida H, Otsuka M, Hoshida Y, Ogura K, Maeda S, Ohmae T, Yanai A, Mitsuno Y, Seki N, Kawabe T, Omata M. NF-kappaB and ERK-signaling pathways contribute to the gene expression induced by cag PAI-positive-Helicobacter pylori infection. *World J Gastroenterol.* **11**, 6134-43 (2005).

[32] Tegtmeyer N, Wessler S, Backert S. Role of the cag-pathogenicity island encoded type IV secretion system in Helicobacter pylori pathogenesis. *FEBS J*. **278**, 1190-202 (2011). Review.

[33] Cendron, L., & Zanotti, G. Structural and functional aspects of unique type IV secretory components in the Helicobacter pylori cag-pathogenicity island. *FEBS J*. **278**, 1223-31 (2011).

[34] Poursina F, Faghri J, Moghim S, Zarkesh-Esfahani H, Nasr-Esfahani B, Fazeli H, Hasanzadeh A, Safaei HG. Assessment of cagE and babA mRNA expression during morphological conversion of Helicobacter pylori from spiral to coccoid. *Curr. Microbiol.* **66**, 406-13 (2012).

[35] Itoh H, Komatsuda A, Wakui H, Miura AB, Tashima Y. Mammalian HSP60 is a major target for an immunosuppressant mizoribine.
J. Biol. Chem. **274**, 35147-35151. (1999)

[36] Miyazaki T, Sagawa R, Honma T, Noguchi S, Harada T, Komatsuda A, Ohtani H, Wakui H, Sawada K, Otaka M, Watanabe S, Jikei M, Ogawa N, Hamada F, Itoh H.73-kDa Molecular Chaperone HSP73 is a Direct Target of Antibiotic Gentamicin. *J. Biol. Chem.* **279**, 17295-17300. (2004).

[37] Yamaguchi H, Osaki T, Takahashi M, Taguchi H, Kamiya S. Colony formation by *Helicobacter pylori* after long-term incubation under anaerobic conditions. *FEMS Microbiol Lett.* **175**, 107-11 (1999).